LAWRENCE
LIVERMORE
NATIONAL
LABORATORY

LLNL-JRNL-639776

Methods to compute dislocation line tension energy and force in anisotropic elasticity

S. Aubry, S. P. Fitzgerald, A. Arsenlis

June 24, 2013

Modelling and Simulation in Materials Science and Engineering

Disclaimer

Methods to compute dislocation line tension energy and force in anisotropic elasticity

S. Aubry[1], S.P. Fitzgerald[2] and A. Arsenlis[1]

[1]*Lawrence Livermore National Laboratory, Livermore, CA, USA.*
[2]*Department of Materials, University of Oxford, Parks Road, Oxford, OX1 3PH UK*

Abstract

A frame indifferent formulation of the energy and force on a dislocation in line tension model in an anisotropic elasticity medium is presented. This formulation is valid for any dislocation line direction and Burgers' vector, and expresses the energy and force in terms of an integral for which no general analytical solution can be calculated. Three numerical methods are investigated to evaluate the energy and the force: direct integration, spherical harmonics expansions and an interpolation table method. We analyze the convergence and computational cost of each method, and compare them with a view to selecting the most appropriate for implementation in large scale dislocation dynamics codes.

1 Introduction

Some dislocation interactions *e.g.* bow-out, cross-slip and junction formation are well-captured by computing only an approximation of the total force on the dislocation. This approximation, the orientation-dependent line tension model, represents dislocations as flexible strings. It assumes a simple energy per unit length of dislocation line and neglects the interactions between dislocations. It has been used to compute the critical stress at which a dislocation bows out [1] and to determine the shape of a dislocation glide loop at equilibrium [2] for general anisotropy. It has also proven effective in determining binary dislocation interactions as a function of their angle of incidence [3, 4, 5, 6, 7].

Line tension expressions for the force and the energy in anisotropic elasticity have been derived by Bacon *et al.* in [11]. In sections 2 and 4 respectively, we revisit the formulation of energy and force in the line tension approximation, and rewrite the expressions in a coordinate-independent form. The formulation proposed by Bacon *et al.* [11] is extended to all Burgers' vectors and

line directions instead of being defined only in the plane containing the line direction of the dislocation and its Burgers vector.

The cost of computing energy in the line tension model is not negligible. A comparison is made between three methods of evaluating the energy and the force: a direct integration method (section 3.1), a spherical harmonics expansion (section 3.2) and an interpolation table method (section 3.3). We study the cost and accuracy of each method as a function of the anisotropy ratio (defined as $A = C_{44}/C'$ in cubic crystals) to determine which one is most suitable for implementation in large scale dislocation dynamics codes.

2 Energy in anisotropic elasticity

The strain energy per unit length of dislocation line in anisotropic elasticity is given in Bacon, Barnett and Scattergood [11] by

$$\mathcal{E} = E \ln\left(\frac{R}{a}\right)$$

where R and a are the inner and outer cut-off radii, and E is the pre-logarithmic energy factor given by

$$E = b_i B_{ij} b_j.$$

E is uniquely determined by the Burgers vector $\boldsymbol{b}$ of the dislocation line, and the 3×3 matrix $\boldsymbol{B}$ given by

$$B_{ij} = \frac{1}{4\pi^2} \int_0^\pi \left[(mm)_{ij} - (mn)_{ir} (nn)^{-1}_{rk} (nm)_{kj} \right] \mathrm{d}\omega \tag{1}$$

where the unit vectors $\boldsymbol{m}$ and $\boldsymbol{n}$ are orthogonal to $\boldsymbol{t}$, the dislocation line direction. The notation $(\boldsymbol{mm})$ is such that $(mm)_{jk} = m_i C_{ijkl} m_l$ where C_{ijkl} is the fourth order elasticity tensor. E has the property that, $E(\boldsymbol{b}, \boldsymbol{t}) = E(-\boldsymbol{b}, -\boldsymbol{t}) = E(-\boldsymbol{b}, \boldsymbol{t}) = E(\boldsymbol{b}, -\boldsymbol{t})$.

In Bacon, Barnett and Scattergood [11], Eq. (1) and its derivatives are given as angular derivatives of the line direction $\boldsymbol{t}$ with respect to an angle between the line direction $\boldsymbol{t}$ and some arbitrary fixed direction. Typically, these angular derivatives are planar: they are defined in the plane containing the line direction $\boldsymbol{t}$ and the fixed direction, usually taken to be the Burgers vector $\boldsymbol{b}$. When $\boldsymbol{b}$ is parallel to the line direction $\boldsymbol{t}$ (*i.e.* a pure screw), the derivatives become ill-defined. To determine line tension forces for all directions in space, another definition is required.

If we define the matrix $\boldsymbol{D}$, such that $\boldsymbol{D} \equiv \boldsymbol{I} - \boldsymbol{t} \otimes \boldsymbol{t}$, where $\boldsymbol{I}$ is the identity matrix, the rows of $\boldsymbol{D}$ correspond to a set of vectors orthogonal to $\boldsymbol{t}$. Define

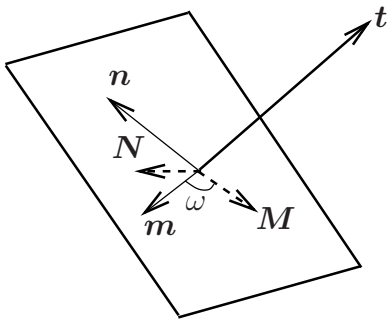

Fig. 1. Notation for energy and force formula in anisotropic elasticity. $\boldsymbol{t}$ is the line direction, ($\boldsymbol{M}$, $\boldsymbol{N}$) are two unit vectors orthogonal to $\boldsymbol{t}$ and ($\boldsymbol{m}, \boldsymbol{n}$) are two unit vectors rotating around ($\boldsymbol{M}$, $\boldsymbol{N}$) with an angle ω and orthogonal to $\boldsymbol{t}$.

α such that

$$D_{\alpha j} = \max_i |D_{ij}|. \tag{2}$$

$\boldsymbol{D}_\alpha$ is one non-vanishing vector orthogonal to $\boldsymbol{t}$ that can always be defined. N_i then is defined as the normalized vector

$$N_i = \frac{D_{i\alpha}}{|D_{i\alpha}|}$$

By construction, $\boldsymbol{t}$ and $\boldsymbol{N}$ are orthonormal, and $\boldsymbol{N}$ is defined independently of the Burgers vector $\boldsymbol{b}$. Defining $\boldsymbol{M} = \boldsymbol{N} \times \boldsymbol{t}$, we have two unit vectors ($\boldsymbol{M}$, $\boldsymbol{N}$) orthogonal to $\boldsymbol{t}$ that are well-defined for all orientations.

Similarly to Bacon *et al.* [11], the two orthogonal unit vectors $\boldsymbol{m}$ and $\boldsymbol{n}$ can be defined by

$$\begin{aligned} \boldsymbol{m} &= \cos\omega\, \boldsymbol{M} + \sin\omega\, \boldsymbol{N} \\ \boldsymbol{n} &= -\sin\omega\, \boldsymbol{M} + \cos\omega\, \boldsymbol{N} \end{aligned} \tag{3}$$

where ω is an angle that varies in $[0, \pi]$ (see Fig. 1). In Bacon *et al.* [11], only $\boldsymbol{M}$ depends on $\boldsymbol{t}$, $\boldsymbol{N}$ does not. In the definitions of Eqs. (3), both $\boldsymbol{M}$ and $\boldsymbol{N}$ depend on the line direction $\boldsymbol{t}$.

3 Methods to compute the energy

Aside from the first term in Eq. (1), the matrix $\boldsymbol{B}$ cannot be computed analytically. Several numerical methods can be used to approximate its calculation. A direct integration using trapezoidal integration, spherical harmonic expansions of $\boldsymbol{B}$, and interpolation methods are among the fastest techniques that can be used to evaluate $\boldsymbol{B}$.

The first term of the integral on the right hand side can be determined analytically. It equals

$$\int_0^\pi \boldsymbol{mm}\,\mathrm{d}\omega = \frac{\pi}{2}(\boldsymbol{MM} + \boldsymbol{NN}).$$

The other term cannot be determined analytically (it involves a quotient of polynomials of order 4 in the numerator and 6 in the denominator). Instead, the energy in anisotropic elasticity can be computed by integrating the remaining terms in Eq. (1) using a numerical method such as trapezoid integration.

The accuracy in the energy calculations depends on the number of angles ω at which the integrand of $\boldsymbol{B}$ is evaluated, and on the anisotropy ratio of the material. The energy does not depend on the length of the dislocation segment considered.

3.2 Spherical harmonics expansion methods

Another way to compute $\boldsymbol{B}$ is to expand it in a spherical harmonics series as

$$\boldsymbol{B} = \sum_{l=0}^{\infty} \sum_{m=-l}^{l} \boldsymbol{B}^{lm} Y_l^m(\boldsymbol{t}) \tag{4}$$

which, by definition, uniformly converges on the unit sphere [12].

The spherical harmonics Y_l^m are defined as the complex functions

$$Y_l^m(\theta, \phi) = M_l^m e^{im\phi} P_l^m(\cos\theta)$$

where $M_l^m = \sqrt{\frac{(2l+1)}{4\pi}\frac{(l-m)!}{(l+m)!}}$, $P_l^m(\cos\theta)$ are the associated Legendre polynomials [13] and (θ, ϕ) are the spherical coordinates of $\boldsymbol{t}$.

The expansion coefficients B_{ij}^{lm} are independent of the line direction $\boldsymbol{t}(\theta, \phi)$ and are defined as

$$B_{ij}^{lm} = \int_0^{2\pi}\int_0^{\pi} B_{ij}(\theta, \phi) Y_l^{m*}(\theta, \phi)\,\sin\theta\,\mathrm{d}\theta\mathrm{d}\phi.$$

where Y_l^{m*} is the complex conjugate of Y_l^m. The coefficients B_{ij}^{lm} can thus be pre-calculated independently of $\boldsymbol{t}$, and stored.

3.2.1 *Spherical harmonics series expansion using recurrence relation of the associated Legendre polynomials (method I)*

A recurrence relation for the associated Legendre polynomials is used to compute the matrix $\boldsymbol{B}$. Since only the even values of l in Eq. (4) give non vanishing values of $\boldsymbol{B}^{lm}$, the following recurrence relation on even l can be used

$$\begin{aligned} P_{\ell+2}^{\ell+2}(z) &= (1-z^2)(2\ell+1)(2\ell+3)P_\ell^\ell(z) \\ P_{\ell+2}^{\ell+1}(z) &= -z\sqrt{1-z^2}(2\ell+1)(2\ell+3)P_\ell^\ell(z) \\ P_{\ell+2}^{m}(z) &= \frac{-1}{(\ell+m+3)(\ell-m+2)}\left[\frac{2(m+1)z}{\sqrt{1-z^2}}P_{\ell+2}^{m+1}(z) + P_{\ell+2}^{m+2}(z)\right] \end{aligned} \tag{5}$$

where $z = \cos\theta$ and θ is one of the angles (θ, ϕ) of the spherical coordinates of the line direction $\boldsymbol{t}$ of the dislocation considered. The initial term of the recurrence is $P_0^0(z) = 1$.

The recurrence relations for the associated Legendre polynomials, and the term $e^{im\phi}$ in the definition of Y_l^m, need to be computed for each dislocation segment, since they depend on the orientation of the line.

3.2.2 *Spherical harmonics series expansion using pre-calculated functions (method II)*

Another implementation using spherical harmonics involves pre-calculating a part of the associated Legendre polynomials. Take the matrix $\boldsymbol{B}$ decomposed in a spherical harmonic series (Eq. (4)); after several expansions and simplifications, it can be written as

$$B_{ij}(\boldsymbol{L}) = \sum_{l=0}^{\infty}\sum_{m=0}^{l}\sum_{k=0}^{[(l-m)/2]} \Re\left[Q_l^m(k)B_{ij}^{lm}(\boldsymbol{t}\cdot\boldsymbol{e_1}\boldsymbol{e_2})^m(\boldsymbol{t}\cdot\boldsymbol{e_3})^{l-m-2k}\right] \tag{6}$$

where $\Re(x)$ denotes the real part of x. The coefficients Q are defined as $Q_l^0(k) = \bar{Q}_l^0(k)$ when $m = 0$ and $Q_l^m(k) = 2\bar{Q}_l^m(k)$, when $m > 0$ with

$$\bar{Q}_l^m(k) = \frac{(-1)^{m+k}}{4\pi^2}\frac{m!}{2^l}\sqrt{\frac{(2l+1)}{4\pi}\frac{(l-m)!}{(l+m)!}}\begin{pmatrix} l \\ k \end{pmatrix}\begin{pmatrix} 2l-2k \\ l \end{pmatrix}\begin{pmatrix} l-2k \\ m \end{pmatrix}$$

The definition of $\boldsymbol{B}$ in Eq. (6) involves a product of terms that depends only on the two variables m and $l-2k$ and can be simplified further

$$B_{ij}(\boldsymbol{t}) = \sum_{q=0}^{\infty}\sum_{m=0}^{2q} \Re\left[S_{ij}^{qm}(\boldsymbol{t}\cdot\boldsymbol{e_1}\boldsymbol{e_2})^m(\boldsymbol{t}\cdot\boldsymbol{e_3})^{2q-m}\right] \tag{7}$$

where S_{ij}^{qm} is a sum of products composed of $Q_l^m(k)$ and B_{ij}^{lm} and is independent of $\boldsymbol{t}$, so it can be pre-calculated independently of $\boldsymbol{t}$. Only the terms of the form $(\boldsymbol{t}\cdot\boldsymbol{e_{12}})^m(\boldsymbol{t}\cdot\boldsymbol{e_3})^{2q-m}$ depend on $\boldsymbol{t}$ in this expression.

3.3 Interpolation using look-up tables

As noted earlier, the matrix $\boldsymbol{B}$ depends only on the line direction of a given dislocation segment and not on its length. Another way of evaluating the matrix $\boldsymbol{B}$ is to pre-calculate its values on the half-sphere defined by $\theta \in [0,\, \pi/2]$ and $\phi \in [0,\, 2\pi]$ and then use an interpolation scheme to approximate the value of $\boldsymbol{B}$ at the spherical coordinates of $\boldsymbol{t} = \boldsymbol{t}(\theta, \phi)$. By symmetries of $\boldsymbol{B}$, $\boldsymbol{B}(\boldsymbol{t}) = \boldsymbol{B}(-\boldsymbol{t})$, only the half-sphere must be considered.

Let $(\theta_i,\, \phi_j)$ be the uniformly distributed grid of $n_\theta \times n_\phi$ angles on the unit half-sphere. The distance between two angles is denoted $\delta\theta = \theta_1 - \theta_0$ and $\delta\phi = \phi_1 - \phi_0$.

The linear interpolation (interpolation of order $d = 1$) for $\boldsymbol{B}(\theta, \phi)$ is

$$\begin{aligned}\boldsymbol{B}(\theta,\phi) = {} & (1-p)(1-q)\boldsymbol{B}(\theta_i,\phi_j) + (1-p)q\boldsymbol{B}(\theta_i,\phi_{j+1}) + \\ & p(1-q)\boldsymbol{B}(\theta_{i+1},\phi_j) + pq\boldsymbol{B}(\theta_{i+1},\phi_{j+1}),\end{aligned}$$

where $i = \frac{\theta}{\delta\theta}$ and $j = \frac{\phi}{\delta\phi}$, $p = i - [i]$ and $q = j - [j]$, with $[i]$ the largest previous integer of i.

For the same i, j, p and q, the interpolation of order d to $\boldsymbol{B}(\theta, \phi)$ is given by

$$\boldsymbol{B}(\theta,\phi) = \boldsymbol{v}(p)\boldsymbol{A}^{-1}\boldsymbol{B}^{\mathbf{g}}\boldsymbol{A}^{-1'}\boldsymbol{v}(q), \tag{8}$$

where the vector $\boldsymbol{v}$ is defined by $v_m(p) = p^{d-m+1}$, the matrix $\boldsymbol{A}$ is defined by

$$A_{m(d-n)} = (m-1)^{n-1}, \tag{9}$$

where the notation $\boldsymbol{A}^{-1'}$ is the transpose of the inverse of $\boldsymbol{A}$. The matrix $\boldsymbol{B^g}$ is the $(d+1)\times(d+1)$ matrix defined as

$$\boldsymbol{B}^{\boldsymbol{g}}_{m,n} = \boldsymbol{B}(\theta_{i+m}, \phi_{j+n})$$

Interpolation methods require only a few matrix-matrix and matrix-vector operations which makes them fast. Their main drawback is the necessity of storing the grid of values $\boldsymbol{B}(\theta_i, \phi_j)$, a set of $n_\theta \times n_\phi$ values.

4 Line tension force

In the dislocation dynamics code ParaDiS [9], dislocations are discretized into straight segments, and forces are defined at the end nodes of these segments. In a line tension calculation, the force at the end node of a segment is the derivative of the energy with respect to this node position. For a dislocation segment $\boldsymbol{L} = \boldsymbol{x} - \boldsymbol{x_1}$, it is given by

$$\begin{aligned}\boldsymbol{F}(\boldsymbol{x}) &= \frac{\mathrm{d}(EL)}{\mathrm{d}\boldsymbol{x}} \\ &= \frac{\mathrm{d}E}{\mathrm{d}\boldsymbol{t}}\frac{\mathrm{d}\boldsymbol{t}}{\mathrm{d}\boldsymbol{x}}L + E\frac{\mathrm{d}L}{\mathrm{d}\boldsymbol{x}} \\ &= \frac{\mathrm{d}E}{\mathrm{d}\boldsymbol{t}} - \left(\frac{\mathrm{d}E}{\mathrm{d}\boldsymbol{t}}\cdot\boldsymbol{t}\right)\boldsymbol{t} + E\boldsymbol{t}\end{aligned} \tag{10}$$

where L is the segment length.

In terms of the matrix $\boldsymbol{B}$, the pre-logarithmic force factor is

$$\boldsymbol{F} = b_i\left[\frac{\mathrm{d}B_{ij}}{\mathrm{d}\boldsymbol{t}}(\boldsymbol{I} - \boldsymbol{t}\otimes\boldsymbol{t}) + B_{ij}\boldsymbol{t}\right]b_j, \tag{11}$$

and the line tension force on the end node $\boldsymbol{x}$ is given by

$$\mathcal{F}^{\mathrm{LT}} = \boldsymbol{F}\log\left(\frac{R}{a}\right).$$

We need to compute the pre-logarithmic force factor $\boldsymbol{F}$ defined in Eqs. (10-11).

4.1 The derivative of energy with respect to the line direction

The line tension force involves the matrix $\mathrm{d}\boldsymbol{B}/\mathrm{d}\boldsymbol{t}$ which needs to be determined in the same basis ($\boldsymbol{t}$, $\boldsymbol{M}$, $\boldsymbol{N}$) described before (Fig. 1). It is given by

$$\begin{aligned}\frac{\mathrm{d}\boldsymbol{B}}{\mathrm{d}\boldsymbol{t}} = &\frac{1}{4\pi^2}\int_0^\pi \frac{\mathrm{d}(mm)_{ij}}{\mathrm{d}\boldsymbol{t}}\mathrm{d}\omega - \\ &\frac{1}{4\pi^2}\int_0^\pi \left[\left(\frac{\mathrm{d}m_u}{\mathrm{d}\boldsymbol{t}}C_{uirs}n_s + m_uC_{uirs}\frac{\mathrm{d}n_s}{\mathrm{d}\boldsymbol{t}}\right)(nn)^{-1}_{rk}(nm)_{kj} - \\ &(mn)_{ir}\left((nn)^{-1}\frac{\mathrm{d}(nn)}{\mathrm{d}\boldsymbol{t}}(nn)^{-1}\right)_{rk}(nm)_{kj} + \\ &(mn)_{ir}(nn)^{-1}_{rk}\left(\frac{\mathrm{d}n_u}{\mathrm{d}\boldsymbol{t}}C_{ukjs}m_s + m_uC_{ukjs}\frac{\mathrm{d}n_s}{\mathrm{d}\boldsymbol{t}}\right)\Bigg]\mathrm{d}\omega\end{aligned} \tag{12}$$

Note that the first term in the integral can be computed analytically

$$\int_0^\pi \frac{\mathrm{d}(\boldsymbol{mm})}{\mathrm{d}\boldsymbol{t}}\mathrm{d}\omega = \frac{\pi}{2}\left[\left(\frac{\mathrm{d}\boldsymbol{M}}{\mathrm{d}\boldsymbol{t}}\boldsymbol{M}\right) + \left(\boldsymbol{M}\frac{\mathrm{d}\boldsymbol{M}}{\mathrm{d}\boldsymbol{t}}\right) + \left(\frac{\mathrm{d}\boldsymbol{N}}{\mathrm{d}\boldsymbol{t}}\boldsymbol{N}\right) + \left(\boldsymbol{N}\frac{\mathrm{d}\boldsymbol{N}}{\mathrm{d}\boldsymbol{t}}\right)\right],$$

where a product of the type $\left(\frac{\mathrm{d}\boldsymbol{M}}{\mathrm{d}\boldsymbol{t}}\boldsymbol{M}\right)$ follows the convention $(\frac{\mathrm{d}M}{\mathrm{d}t_p}M)_{jkp} = \frac{\mathrm{d}M_i}{\mathrm{d}t_p}C_{ijkl}M_l$.

The derivatives of the vectors $\boldsymbol{m}$ and $\boldsymbol{n}$ are given in terms of the derivatives of $\boldsymbol{M}$ and $\boldsymbol{N}$ with respect to the line direction by

$$\begin{aligned}\frac{\mathrm{d}\boldsymbol{m}}{\mathrm{d}\boldsymbol{t}} &= \cos\omega\,\frac{\mathrm{d}\boldsymbol{M}}{\mathrm{d}\boldsymbol{t}} + \sin\omega\,\frac{\mathrm{d}\boldsymbol{N}}{\mathrm{d}\boldsymbol{t}}\\ \frac{\mathrm{d}\boldsymbol{n}}{\mathrm{d}\boldsymbol{t}} &= -\sin\omega\,\frac{\mathrm{d}\boldsymbol{M}}{\mathrm{d}\boldsymbol{t}} + \cos\omega\,\frac{\mathrm{d}\boldsymbol{N}}{\mathrm{d}\boldsymbol{t}},\end{aligned} \tag{13}$$

and those of $\boldsymbol{M}$ and $\boldsymbol{N}$ by

$$\begin{aligned}\frac{\mathrm{d}N_i}{\mathrm{d}t_j} &= \frac{N_iN_jt_\alpha}{\sqrt{1-t_\alpha^2}} - \frac{(\delta_{ij}t_\alpha + \delta_{\alpha j}t_i)}{\sqrt{1-t_\alpha^2}}\\ \frac{\mathrm{d}M_i}{\mathrm{d}t_j} &= \frac{\epsilon_{i\alpha j} - M_iN_jt_\alpha}{\sqrt{1-t_\alpha^2}}\end{aligned} \tag{14}$$

since $|D_\alpha| = \sqrt{1-t_\alpha^2}$. Note that in the previous expressions (Eqs. (14)), there is no sum on the index α as it is fixed by Eq. (2) and t_α is the α component of the line direction $\boldsymbol{t}$.

Combining Eqs. (13) and (14), the derivative of the matrix $\boldsymbol{B}$ given in Eq. (12) is fully determined.

4.2 Spherical harmonics expansion of the line tension force

The line tension force, like the energy, can be decomposed in spherical harmonics. Two methods can be used to express it: one uses the recurrence relation for the associated Legendre polynomials, and the other pre-calculates as many terms in the expansion as possible to reduce the cost of its calculations.

4.2.1 *Spherical harmonics series expansion using recurrence of the associated Legendre polynomials, (method I)*

The chain rule for the derivative of the spherical harmonics expansion of $\boldsymbol{B}$, Eq. (4) can be used to derive a recurrence relation for the line tension force, Eq. (11). It is given by

$$\frac{\mathrm{d}\boldsymbol{B}}{\mathrm{d}\boldsymbol{t}} = \sum_{l=0}^{\infty}\sum_{m=-l}^{l} \boldsymbol{B}^{lm}\left[imY_l^m(t)\frac{\partial\phi}{\partial\boldsymbol{t}} + M_l^m e^{im\phi}P_l^{m'}(z)\frac{\partial z}{\partial\boldsymbol{t}}\right]$$

where we have posed $z = \cos\theta$ and where $P_l^{m'}(z)$ is the derivative of the Legendre polynomial $P_l^m(z)$ with respect to z.

Using the following identity for the associated Legendre polynomials

$$(z^2-1)P_l^{m'}(z) = \sqrt{1-z^2}P_l^{m+1}(z) + mzP_l^m(z),$$

and that the derivatives of the spherical coordinate ϕ and $z = \cos\theta$ are

$$\frac{\partial\phi}{\partial\boldsymbol{t}} = \frac{(\boldsymbol{t}\cdot\boldsymbol{e_x})\boldsymbol{e_y} - (\boldsymbol{t}\cdot\boldsymbol{e_y})\boldsymbol{e_x}}{(\boldsymbol{t}\cdot\boldsymbol{e_x})^2 \;+\; (\boldsymbol{t}\cdot\boldsymbol{e_y})^2} = \frac{\cos\phi\,\boldsymbol{e_y} - \sin\phi\,\boldsymbol{e_x}}{\sin\theta}$$

and

$$\frac{\partial z}{\partial\boldsymbol{t}} = -(\sqrt{1-z^2})\boldsymbol{e_z},$$

we obtain

$$\frac{\mathrm{d}\boldsymbol{B}}{\mathrm{d}\boldsymbol{t}} = \sum_{l=0}^{\infty}\sum_{m=-l}^{l} \boldsymbol{B}^{lm}M_l^m\left[\left(i\frac{\partial\phi}{\partial\boldsymbol{t}} - \frac{z}{\sqrt{1-z^2}}\boldsymbol{e_z}\right)mP_l^m(z) - P_l^{m+1}(z)\boldsymbol{e_z}\right]e^{im\phi}$$

The same relation of recurrence as Eqs. (6) can be used to compute the polynomials P_l^m and the calculation of $\frac{\mathrm{d}\boldsymbol{B}}{\mathrm{d}\boldsymbol{t}}$ follows.

4.2.2 *Spherical harmonics series expansion using pre-calculated functions (method II)*

Differentiating the spherical harmonic expansion for $\boldsymbol{B}$ in Eq. (7) gives

$$\frac{dB_{ij}}{d\boldsymbol{t}} = \sum_{q=1}^{\infty}\sum_{m=0}^{2q} \Re\left\{S_{ij}^{qm}(\boldsymbol{t}\cdot\boldsymbol{e_{12}})^{m-1}(\boldsymbol{t}\cdot\boldsymbol{e_3})^{2q-m-1}[m(\boldsymbol{t}\cdot\boldsymbol{e_3})\boldsymbol{e_{12}} + (2q-m)(\boldsymbol{t}\cdot\boldsymbol{e_{12}})\boldsymbol{e_3})]\right\} \tag{15}$$

Combining Eqs. (7) and (15), the line tension force given in Eq. (11) is fully determined.

5 Numerical results

When the direct integration method is used, a relative error of 10^{-16} in energy calculations is found for approximately 100 integration angles for any anisotropy ratio. The corresponding energy value is set as a reference value for estimating the relative error in energy calculations for the other methods. The corresponding time to compute this reference energy value is set to t_{ref}. In the next figures, "relative cost" means the computational cost of the method considered t divided by the reference time time t_{ref}, relative cost $= t/t_{\text{ref}}$.

The relative cost of computing the energy for the three methods described in section 3 for a fixed anisotropy ratio of $A = 7.45$ (corresponding to α-Fe at 900℃) is shown in Fig. 2. Fig. 2[a] shows the relative cost for the direct integration method (section 3.1) as well as a linear fit. The relative cost depends on the number of angles ω in $[0, \pi]$ chosen to evaluate the integral. Fig. 2[b] shows the relative cost as a function of the expansion order $q_{\max}$ for the two spherical harmonics methods (sections 3.2.1 and 3.2.2) as well as a quadratic fit.

The relative cost when using the direct method increases linearly as a function of the number of angles, and increases quadratically as a function of the expansion order $q_{\max}$ when using the spherical harmonics methods. The spherical harmonics method I (section 3.2.1) is $1.85 - 2.7$ times more expensive than the spherical harmonics method II (section 3.2.2).

The speed increase from the spherical harmonics method I to method II is a result of the larger number of precalculations done in the spherical harmonics expansion method II. In method I, only the coefficients B_{ij}^{lm} are precomputed. In method II, both the coefficients B_{ij}^{lm} and Q_l^m are precalculated. Also the recurrence relations to calculate the Legendre polynomial is fast but the recurrence relation to obtain the product $(\boldsymbol{t} \cdot \boldsymbol{e_{12}})^m (\boldsymbol{t} \cdot \boldsymbol{e_3})^{2q-m}$ is faster.

The cost of computing the energy in the interpolation method (section 3.3) should depend on the number of grid points $n_\theta \times n_\phi$ and the order of interpolation. Fig. 2[c] shows the relative cost of the interpolation method averaged over the number of angles as well as the standard deviation and a linear fit.

The relative cost of the interpolation method does not depend on the anisotropy ratio nor on the number of grid points chosen to interpolate $\boldsymbol{B}$, since these values are pre-tabulated. Also, it does not appear to vary much with the order of interpolation. As the order of interpolation increases, larger matrices and vectors are involved in the matrix/vector products of Eq. (8) but this is negligible compared to the cost of retrieving the elements of the interpolated grid.

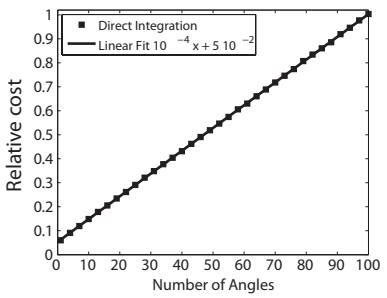

(a) Direct integration

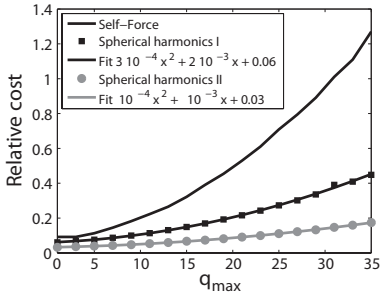

(b) Spherical harmonics

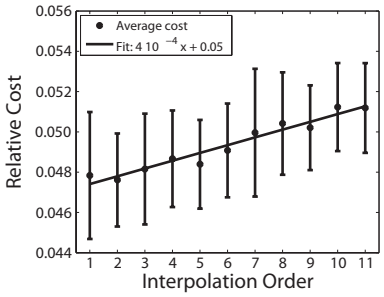

(c) Interpolation method

Fig. 2. Growth of the relative cost of computing the line tension energy using different methods. (a) Linear growth for direct integration with a linear fit of the cost. (b) Quadratic growth for spherical harmonics methods using recurrence for Legendre polynomials (method I) and pre-calculated expansion coefficients (method II) and quadratic polynomial fits. The cost of computing the self-force is also shown. Spherical methods use a fixed anisotropy ratio of $A = 7.45$. (c) Average over the number of angles of the relative cost of the interpolation method as the interpolation order increases and standard deviation. This data is fit to a linear polynomial.

The order of magnitude of the cost of computing the energy can be evaluated by comparing to the cost of computing self-forces. The self force of a dislocation segment is the force due to its own stress field. It has been computed using a spherical harmonics expansion in Aubry and Arsenlis [10]. Fig. 2[b] shows the cost of computing the energy for the line tension model using the two spherical harmonics methods described in Section 3.2. These relative costs are compared to the cost of computing the self-force on the same dislocation segment using spherical harmonics expansions for an anisotropy ratio of $A = 7.45$. This figure shows that line tension calculations are not negligible. The cost of computing line tension using the spherical expansion method II (section 3.2.2) is $3 - 7.5$ times less expensive than computing self-forces.

Fig. 3[a] shows the error in energy calculations as a function of interpolation order and number of grid points for a fixed anisotropy ratio of 7.45. Fig. 3[b] shows the base 10 log of the energy calculations error as a function of the relative cost for a fixed anisotropy ratio and a fixed interpolation order of 11. The interpolation method of order 11 needs about $2,000$ grid points to reach an error in energy calculations of 10^{-7} and about $50,000$ points to reach an error

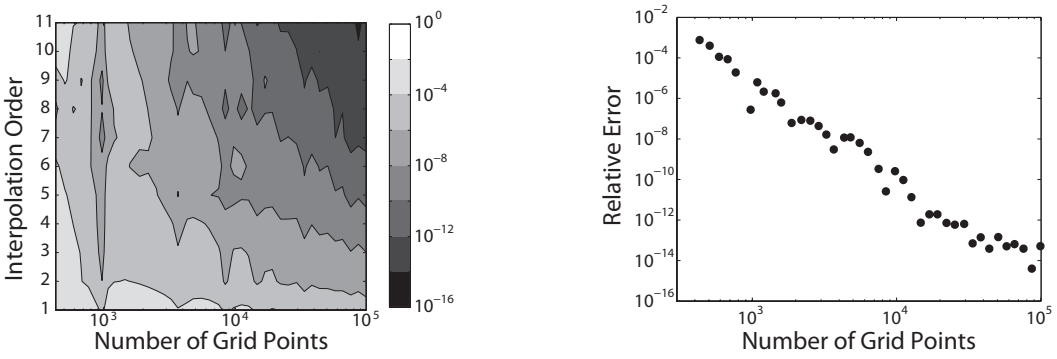

(a) Interpolation method (b) Error in energy calculations

Fig. 3. Energy error calculations for the interpolation method for a fixed anisotropy ratio of $A = 7.45$ (a) as the number of grid points and the order of interpolation increase. (b) For a fix interpolation order of 11, energy calculation error decrease with the number of grid points.

of 10^{-12}. The interpolation method is fast compared to the two other methods but requires a large stored grid to converge. The relative cost of computing the energy using linear interpolation is about 20 times less expensive than the direct method.

Fig. 4 compares the error in energy calculations as a function of cost and anisotropy ratio for the direct integral calculations (Fig. 4[a]), the spherical harmonics method I (Fig. 4[b]) and II (Fig. 4[c]) described in the previous sections and for the interpolation method (Fig. 4[d]). The relative cost represented in Fig. 4 is deduced from Fig 2.

The interpolation method converges faster to a lower error in energy calculation than all the other methods. The spherical harmonics method II is the second fastest and requires much less storage. The error in energy calculation decreases exponentially for the direct integration and the spherical harmonics methods as a function of anisotropy ratio while the error in energy calculations for the interpolation method remains constant.

We have also computed the cost and accuracy of calculating the line tension force at a point for the three numerical methods: direct integration, spherical harmonic expansions and interpolation as a function of anisotropy ratio. The same conclusions seen for energy can be made for forces. Aside from the actual values, the trends are the same. The comparison results for the force error calculations are not shown in this paper.

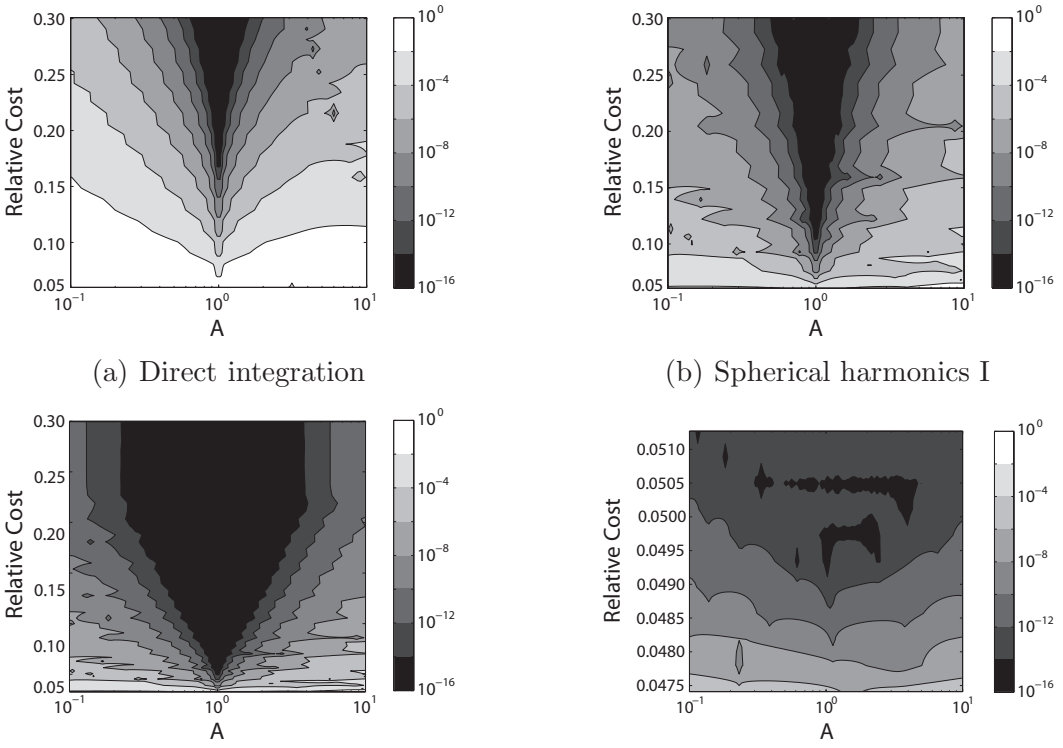

(a) Direct integration

(b) Spherical harmonics I

(c) Spherical harmonics II

(d) Interpolation

Fig. 4. Energy error comparisons for different methods as a function of relative cost and anisotropy ratio. (a) Direct integration. (b) Spherical harmonics method I. (c) Spherical harmonics method II. (d) Interpolation methods for a number of $47,000$ grid points.

6 Conclusion

A coordinate-independent line tension formulation for the dislocation energy and force has been proposed for anisotropic elasticity. The expressions for the energy and its derivative are extended and are valid for dislocation line directions that can vary anywhere on the unit sphere. They are not limited to a plane containing the line direction and a fixed direction.

Three methods have been investigated to compute the energy in the line tension model in an anisotropic elastic medium. Choosing which method is the most cost efficient and accurate depends on the problem to be solved and the accuracy desired.

The direct integration method needs about $40 - 50$ angles about the target line direction to reach a precision of $10^{-7} - 10^{-16}$ in energy, depending on the anisotropy ratio. It does not use any stored values, except perhaps the sines and cosines of the integration angles which can be pre-computed and stored and elastic constants.

The two spherical harmonics methods converge faster per unit computational cost than the direct method. As the anisotropy ratio gets further away from one, the spherical harmonics method becomes more expensive since the accuracy grows quadratically with $q_{\max}$. It also needs to store more data than the direct integration method (such as the S_{ij}^{qm} coefficients described in the text). These coefficients represent $9(q_{\max}+1)(q_{max}+2)$ real values. For $q_{\max}=10$, it is about $1,200$ values and for $q_{\max}=20$, this is about $4,200$ values.

The least computationally expensive method is the high order interpolation method. It requires approximately 1/20 of the relative cost to reach an accuracy of about 10^{-13} in energy error calculations but it requires the storage of angular grid points ($50,700$ values corresponding to 130×390 angle pairs), the storage of the interpolation matrix A (Eq. (9)) and evaluations of $\boldsymbol{B}$ to converge to this precision. The interpolation method can be used if storage of the grid points is not a problem, for instance the case of small simulations involving only a few dislocations on a single processor.

There are advantages and drawbacks in using any of these methods and it might be useful to switch from one method to the other for a given problem. The spherical harmonics method (method II) is a good compromise between low relative cost and storage.

Acknowledgments

Lawrence Livermore National Laboratory is operated by Lawrence Livermore National Security, LLC, for the U.S. Department of Energy, National Nuclear Security Administration under Contract DE-AC52-07NA27344.

References

[1] S. Fitzgerald, S. Aubry, S. Dudarev, and W. Cai. Discrete dislocation dynamics simulation of frank-read sources in anisotropic alpha-fe. *Modelling and Simulation in Materials Science and Engineering*, 2012.

[2] S. Aubry, S. Fitzgerald, S. Dudarev, and W. Cai. Equilibrium shapes of dislocation shear loops in anisotropic alpha-fe. *Modelling and Simulation in Materials Science and Engineering*, 19:065006, 2011.

[3] L. Dupuy and M. C. Fivel. A study of dislocation junctions in fcc metals by an orientation dependent line tension model. *Acta Materialia*, 50(19):4873 – 4885, 2002.

[4] LP Kubin, R Madec, and B Devincre. Dislocation intersections and reactions in FCC and BCC crystals. In Zbib, HM and Lassila, DH and

Levine, LE and Hemker, KJ, editor, *Multiscale phenomena in materials-experiments and modeling related to mechanical behavior*, volume 779, pages 25–36. Mat Res Soc, Materials research society, 2003.

[5] R Madec, B Devincre, and LP Kubin. On the nature of attractive dislocation crossed states. *Computational materials science*, 23(1-4):219–224, 2002.

[6] LK Wickham, KW Schwarz, and JS Stolken. Rules for forest interactions between dislocations. *Physical review letters*, 83(22):4574–4577, 1999.

[7] G. Monnet, B. Devincre, and L. P. Kubin. Dislocation study of prismatic slip systems and their interactions in hexagonal close packed metals: application to zirconium. *Acta Materialia*, 52(14):4317 – 4328, 2004.

[8] J.P. Hirth and J. Lothe. *Theory of Dislocations.* Krieger publishing company, 1982.

[9] A Arsenlis, W Cai, M Tang, M Rhee, T Oppelstrup, G Hommes, T G Pierce, and V V Bulatov. Enabling strain hardening simulations with dislocation dynamics. *Modelling and Simulation in Materials Science and Engineering*, 15(6):553–595, 2007.

[10] S. Aubry and A. Arsenlis. Use of spherical harmonics for dislocation dynamics in anisotropic elastic media. Submitted to MSMSE 2013.

[11] D.J. Bacon, D.M. Barnett, and R.O. Scattergood. Anisotropic continuum theory of lattice defects. *Prog. Mater. Sci.*, 23:51–262, 1980.

[12] T. Mura and N. Kinoshita. Green's functions for anisotropic elasticity. *Phys. Stat. Sol. (b)*, 47:607, 1971.

[13] M. Abramowitz and I.A. Stegun. *Handbook of Mathematical Functions: With Formulas, Graphs, and Mathematical Tables : [is an Outgrowth of a Conference on Mathematical Tables Held at Cambridge, Mass., on 1954.* Applied mathematics series. Dover Publ., 1965.

[14] W. Cai, A. Arsenlis, C. R. Weinberger, and V. V. Bulatov. A non-singular continuum theory of dislocations. *Journal of the Mechanics and Physics of Solids*, 54:561, (2006).